International Conference
ENGINEERING MECHANICS 2010
Svratka, Czech Republic, May 10 – 13, 2010

MULTI-FUNCTIONING IN BIOMECHANICS OF LAMINATED WOOD VS CARBON FIBER COMPOSITES

Alexander Tesar*, Ludovit Nasch*

Summary: *Multi-functioning and multi-optimization in the biomechanics of laminated wood vs carbon fiber composites are treated in present paper. Multi-functioning is one of the key features enabling multiple functions to be carried out in laminated wood vs carbon fiber composites and structures with their hierarchical bionics configuration. Theoretical, numerical and experimental assessment of the problem is presented. The application on the shell roof structure designed with multi-function approach suggested is submitted.*

1. Introduction

Although human genius through various inventions makes instruments corresponding to the same ends, it will never discover an invention more beautiful nor more ready nor more economical than does nature, because in her inventions nothing is lacking and nothing is superfluous (Leonardo da Vinci [1]).

One of interesting conclusions of the above statement of da Vinci is that natural organisms from a design point of view need the co-existence of multiple functions in a single component or mechanism. The natural organisms are the set-ups of many sub-systems being integrated together. The nature contains countless multi-functioning systems that are of great relevance to human design. It appears therefore as very useful to study multi-functioning in the nature because the results can be implemented into desirable attributes for design.

Such multi-functioning appears also in laminated wood (GLULAM) vs carbon fiber (RELAM) composites used in advanced structural engineering. Some of the issues considered in the multi-functional design of such structures are mentioned as follows:

Control of forcing

The forcing can be varied by suitable geometry and shape of GLULAM and RELAM composites. For example, the wind turbulences force such structures with a considerable power. The forced movements due to wind turbulence and associated mechanisms are stochastic

* Alexander Tesar, Ing., PhD, DrSc, prof., Ludovit Nasch, Ing., PhD, Institute of Construction and Architecture, Slovak Academy of Sciences, Dubravska cesta 9, 845 03 Bratislava 45, Slovak Republic, usarate@savba.sk

in nature. There appears a strong vortex wake associated with aerodynamic drag force experienced by the body. Depending on the wind speed and the cross-section's shape, the shedding of vortices is more or less regular with shedding periods inversely proportional to the wind speed. In resonant conditions the structure's oscillations control the rhythm of the vortex shedding and limited amplitude vibrations occur. Aside the known vortex trail type excitation the more general types of aerodynamic forcing can appear there. Possible re-attachment of separated flow as well as the vortices generated by the local geometry and movements of the body contribute to aerodynamic forces experienced by the structure. Aerodynamic forces proportional to the movements of the body result in self-induced divergent vibrations at high wind speeds. In theoretical treatment the concepts of aerodynamic damping and aerodynamic stiffness are applied. In the design is to be avoided that absolute value of negative aerodynamic damping force exceeds the positive mechanical damping force producing oscillatory torsion or across-wind flexural mode instability.

Material and structural layout

The hierarchical layout of the material in GLULAM and RELAM composites is optimal from a structural point of view as well as for generating an efficient flow of forces. Besides an hierarchical layout such structures have optimal material and shape properties. Their configuration is efficient for resisting bending and buckling. All structural sections are tapered so that the section size is well matched to the applied loads. The GLULAM and RELAM composites consist of micromechanical fibers and of surface resin skin. The modeling takes into account all interactions of fibers with surface skin and the analysis leads to numerical approaches on the level of micro-mechanics.

Fail-safe mechanisms

The composites studied are equipped with embedded self-healing mechanisms being activated when a crack appears. Such mechanism consists of distributed glue cells within the composite and they are activated when material is overstressed. The local cells are small enough so that overall structural properties are not significantly compromised. The fail-safe mechanisms are adopted in hierarchical configuration of GLULAM and RELAM composites. If the elements are overloaded they unzip from adjacent elements before serious damages occur. The elements can be re-zipped by simple stress redistribution. The large number of zipping mechanisms ensures that the structure will unzip very close to the point of overload, thus causing minimum damage. Similar optimal fail-safe features appear also in glued connections of the composites studied.

Tuned behavior control

In order to ensure the satisfactory composite action between carbon fiber composites and laminated wood the shear connectors have to be placed in the areas of concentrated loads. Such tuning facilities are adopted with regard to three main items as are the changes in stiffness, moment resistance and rotation capacity (ductility). Tuned vibration adopted in dynamic systems contributes to multi-functioning of such composites.

Some another approaches dealing with multi-functioning in reliability analysis, design and application of GLULAM and RELAM composites are discussed, for example, in Refs. [2] and [3].

2. Laminated wood vs carbon fiber composite

Two types of laminated wood are analyzed – the spruce (picea abies) with mechanical properties due to EN 384 and strength class C27 and the oak (quercus robur) with mechanical properties due to the same source and with the strength class D40.

The carbon fiber composite is adopted in strips having thickness 1.3 mm and width 50 mm. The strips are located in one or several shifts in the cross section of the laminated wood specimens studied (see Fig. 1). Tensile strength and Young modulus of the carbon fiber composite suggested are 2300 MPa and 200 GPa, respectively.

The connection of laminated wood with carbon fiber elements is made by epoxy glue with viscosity 600 – 1200 Pa.s at temperature 25˚C.

Theoretical approach suggested is based on the assumption of linear elastic behavior in tensile zones and elastic-plastic action in compression zones of the specimens tested. In compression zones there are considered visco-elastic and visco-plastic properties of the wood adopted. Carbon fiber elements are analyzed under assumption of their linear elastic behavior.

3. Analysis

The model aimed allows the analysis of actual interaction of all elements of GLULAM and RELAM composites studied. The wood members subjected to compression act in linear-elastic behavior until obtaining their ultimate strength. There follows the decrease of the stress level as consequence of increasing deformation. The GLULAM elements subjected to the tension act in linear-elastic response.

For each new location of the neutral axis the load increments in all elements are to be evaluated. All modes of collapse are respected. In the analysis of compression stress occurring in laminated wood elements there appears the plastification with incremental changes of the neutral axis.

Laminated carbon fiber composites have high strength. Under certain circumstances, however, there appear the lateral loads causing the shear delamination in surface regions of the matrix as well as in the inter-laminar zones filled with resin. This leads consequently to the reduction of the strength. Polymer matrices are made of isophtalic polyesters TMR 300 with polyurethan resin. The interlaminar fracture toughness for delamination appears there as significant parameter in the analysis. In addition to the measurement of inter-laminar fracture toughness for delamination of carbon fiber elements there follows their surface analysis adopting the scanning electron microscopy. For numerical treatment of the ultimate strength of the carbon fiber composite the micromechanical models adopting the concept of nano-tubes can be adopted.

When laminated wood specimen with carbon fiber elements consists of densely packed inclusions, their interaction effects may play a significant role in the behavior of the resulting continuum. The concept of transformation strain can be used when an elastic medium contains periodically distributed inclusions or voids in the material. Because of the periodicity, the transformation strains are regular functions of space, time and temperature.

The periodicity is exploited in an effort to obtain accurate estimate for the transformation strains used to approximate mechanical properties of laminated wood vs carbon fiber composite.

The Washizu´s variation principle is adopted in order to include initial stress and strain components due to isothermal deformation in time. The stress in the microelement at the beginning of the time increment studied is considered as initial stress with thermal strain increment. The variation principle adopted is then written in the terms of time rate quantities given by

$$I = \{\int_V [S_{ij}\, \varepsilon_{ij} + 0.5\, W_{ij}\, u_{ki}\, u_{kj} - (\varepsilon^{o}_{ij} + 0.5\, \varepsilon'_{ij})\, S_{ij}]\, dV - \int_{A1} r_i^{(.)}\, u_i\, dA1 - \int_{A2} s_i\, (u_i - w_i)\, dA2\}(dt)^2$$

$$+ \{\int_V W_{ij}\, \varepsilon_{ij}\, dV - \int_{A1} r_i\, u_i\, dA1 - \int_{A2} p_i\, (u_i - w_i)\, dA2\}dt \quad , \quad (1)$$

where W_{ij} and S_{ij} are the Piola-Kirchhoff stress tensors for initial stress and strain rate, respectively, p_i and s_i are the Lagrange surface traction and its time rate quantity, respectively, r_i and $r_i^{(.)}$ are studied on surface area $A1$ and w_i on area $A2$. The volume V is bounded by surface area $A = A1 + A2$. The total strain rate ε_{ij} is composed of the initial strain rates ε^{o}_{ij} and ε'_{ij}, corresponding to instantaneous stress rate S_{ij}. To evaluate the strain rate, the thermal expansion coefficient at temperature T is $\alpha(T)$ and at temperature $T+dT$ is $\alpha(T+dT)$. By expanding $\alpha(T+dT)$ into Taylor series, the average thermal strain rate is obtained.

Identification approach suggested

The covariance matrices adopted for forcing are denoted by $R_x(t_i)$ and $R_{xm}(t_i)$. The relation between covariance matrices $Y(t_i)$ of the process $y(t_k)$ and system matrices F, G and B of the discrete time model is given by

$$Y_k(t_i) = G\, F_{k-1}\, M(t_i) \quad , \quad (2)$$

with

$$M(t_i) = F\, R_x(t_i)\, G^T + B\, R_{xm}(t_i) \quad . \quad (3)$$

The Hankel matrix established by covariance matrices $Y_k(t_i)$ is used in the algorithm of the identification approach suggested by:

1. Form the Hankel matrix of the problem.
2. Compute the singular value decomposition of the Hankel matrix given by

$$H(p) = U\, T^2\, V^T \quad , \quad (4)$$

   with U and V as orthogonal matrices and T as diagonal and semi-definite matrix of singular values.
3. System matrices for the problem studied are given by

$$F = T^{-1}\, U^T\, H(p)\, V \quad , \quad (5)$$
$$M = T\, V^T\, E_n \quad , \quad (6)$$
$$G = E_n\, U\, T \quad , \quad (7)$$

   with

$$E_n = [\, I_n \;\; 0 \;\; 0 \;\; \ldots \;\; 0 \,] \quad . \quad (8)$$

3. Solve the eigenvalue problem established by the (m x m)-upper left submatrix of the (n x n)-system matrix *F*.
5. Compute the modal parameters from the eigenvalues obtained.
6. Repeat operations from step 4 up for increasing system submatrix.

Ultimate response

The Fourier integral transformation combined with the FETM-approach is adopted for the analysis of the ultimate response ([8]). Considered is the load $P_j(t)$ acting on the composite studied. The load is located in node j $(j = 1, 2, 3, \ldots n)$ in time t. The response in node i is given by $X_i(t)$ $(i=1, 2, 3, \ldots m)$. The symbol $g_{ij}(\omega)$ specifies the spectral response function in node i due to the unit impulse $e^{i\omega t}$. There holds

$$X(t) = \int g(t)\, P(t)\, dt \quad , \quad (9)$$

with vectors $X(t)$ and $P(t)$ of the functions $X_i(t)$ and $P_i(t)$, respectively, and with $g(t)$ as (m x m)-matrix of the functions $g_{ij}(\omega)$. Generalized ultimate response is given by

$$M_Y(\omega) = N(\omega)\, M_P(\omega) \quad , \quad (10)$$

where $N(\omega)$ is the complex transfer function of the composite studied and $M_Y(\omega)$ is ultimate response transform of the forcing function $M_P(\omega)$. The complex function of structural response $N(\omega)$ defines the spectral characteristics of the composite. Simultaneously there are specified the amplitude and phase shift of the response related to harmonic components of the ultimate forcing spectrum adopted.

Structural multi-optimization

The multi-optimization is adopted as the selection of design parameters allowing minimum weight or fully stressed design. The selection of design parameters is subjected to following types of constraints:

- geometric constraints – minimum and maximum areas, dimensions and rigidities of structural members adopted,
- stress constraints – maximum stress allowed,
- displacement constraints – minimum and maximum deformations, rotations and displacements,
- resonance, stability and fatigue ultimate constraints.

Such items specify the regional constraints and are applied for all forcing possibly occurring. They are represented by the constraint hyper-surfaces. Stress and deformations as well as resonance, stability and fatigue ultimate limits are the nonlinear functions of the design variables. The constraint hyper-surfaces are also nonlinear functions of such variables. If design point lies above the constraint surfaces then stress and displacements in regional constraints are within the limits specified. The contact of the constant-weight hyper-surface with the constraint hyper-surfaces is the point of the minimum weight design.

When the constraints are imposed only on stress, an iterative procedure is used to re-design the structure so that each element reaches limit stress under at least one of the load conditions assumed. Such design is described as a fully stressed design. The design variables for fully stressed design converge to a vertex of n hyper-surfaces representing the stress constraints.

General multi-optimization approach of the composites studied is stated as follows: Find the geometric design variables Y and the cross-sectional design variables X or Z (as other types of variables) such that holds:

objective function $$W = f(X, Y, Z) \rightarrow min \quad , \quad (11)$$

geometric constraints $$X^L \leq X \leq X^U \quad , \quad (12)$$
$$Y^L \leq Y \leq Y^U \quad , \quad (13)$$
$$Z^L \leq Z \leq Z^U \quad , \quad (14)$$

stress constraints $$\sigma^L \leq \sigma \leq \sigma^U \quad , \quad (15)$$

displacement constraints $$r^L \leq r \leq r^U \quad , \quad (16)$$

resonance, stability and fatigue constraints $$\gamma^L \leq \gamma \leq \gamma^U \quad , \quad (17)$$

with superscripts L und U specifying lower and upper bounds, respectively. The symbols σ, r and γ are stress, displacements, resonance, stability and fatigue limits adopted. Such limits are implicit functions of the design variables adopted. The scope of the straightforward approach is to multi-optimize simultaneously all above variables by one of available nonlinear programming techniques. A possible procedure for such multi-optimization is given by following operations:

1. Assume an initial structural geometry.
2. Optimize cross-sectional variables and forces for given geometry by satisfaction of Eqs. (11) – (17).
3. Modify the geometric variables.
4. Repeat the steps 2 and 3 until optimal structural geometry is obtained.

The number of design variables is reduced by stating all geometric dimensions and parameters in the terms of a small number of independent variables. The design variable linking is often necessary also due to such items as functional requirements, fabrication limits, boundary conditions, temperature, etc. Another possibility to reduce the number of candidate geometries is to use a coarse grid in the space of geometric variables, so that only a small number of X, Y or Z values is to be considered. This is justified in cases where objective function (minimum weight design or fully stressed design) is not sensitive to the changes in geometric variables near the optimum. In order to optimize X, Y and Z variables in this step, one of techniques mentioned for example in references [2], [3] or [4] can be adopted.

4. Experiment

The GLULAM girders reinforced with carbon fiber strips (RELAM) as shown in Fig. 1 were tested. The regions where the assessment of deformations was made are also shown in Fig. 1. The cross-section of the girder is in Fig. 2. The girders (**0**-X) are without carbon fiber

reinforcement (GLULAM). The girders (**I**-X) are equipped with carbon fiber reinforcement in one shift and girder (**II**-X) in two shifts (RELAM).

The reinforcement was made using carbon fiber sheets CarboDur S 512 having elasticity modulus E=165 GPa and total cross-sectional area A=120 mm^2. As example, the girder 0-2 (GLULAM-specimen without reinforcement) is shown in Fig. 3.

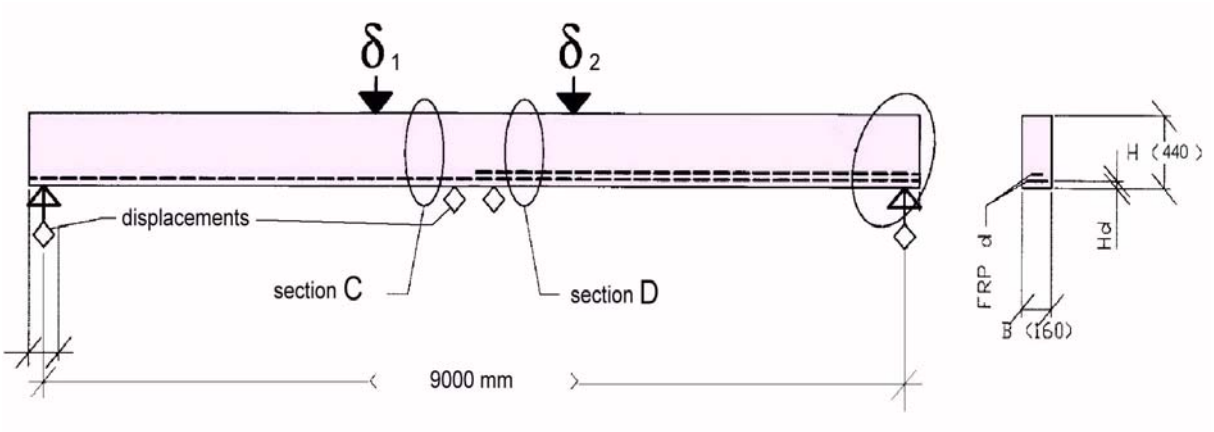

Fig. 1. Scheme of reinforcement in girder with regions measured

Fig. 2. Cross-section of three girders tested (0-X, I-X, II-X)

Fig. 3. View of girder tested ("2" is fixation device)

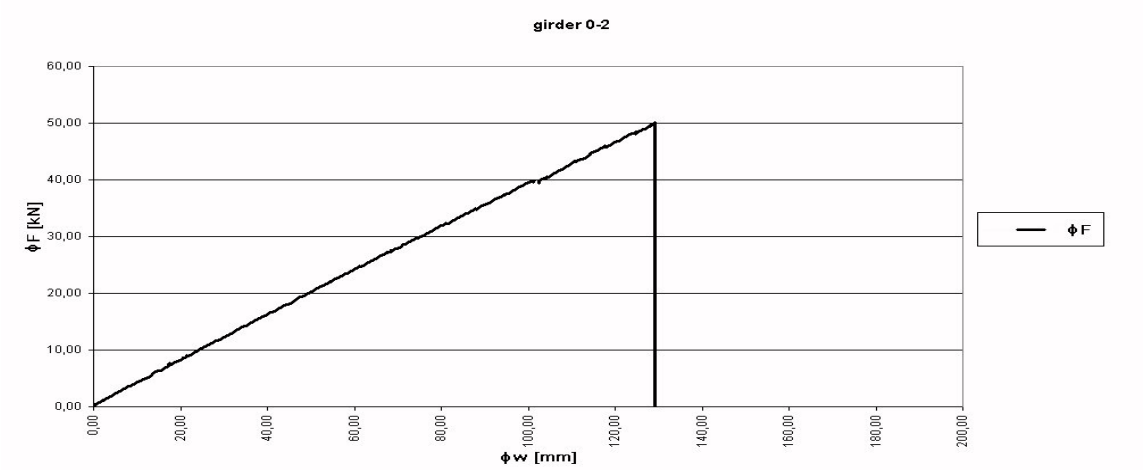

Fig. 4. Force ϕF vs deflection ϕw of the girder 0-2 (GLULAM without reinforcement)

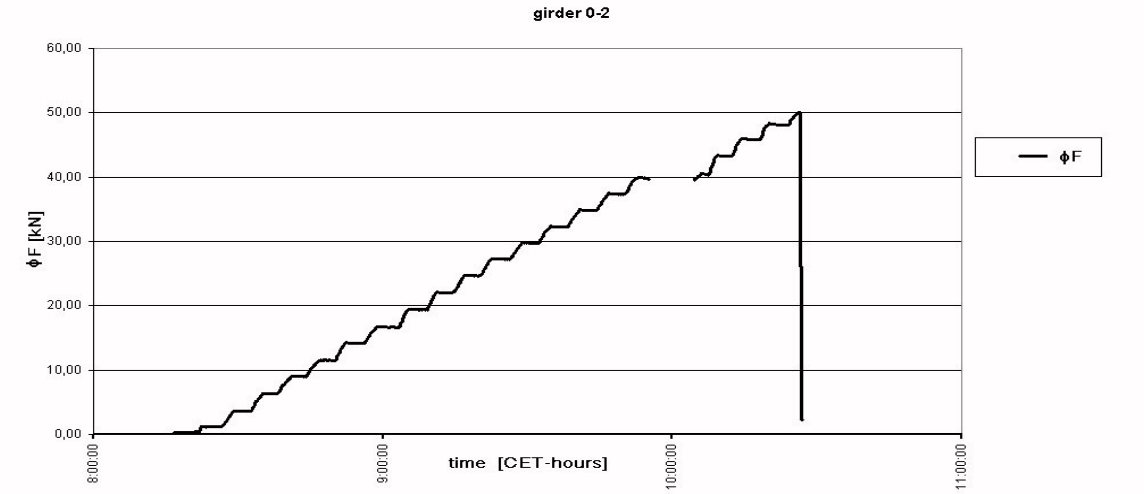

Fig. 5. Force ϕF vs time (CET) in girder 0-2 (without reinforcement)

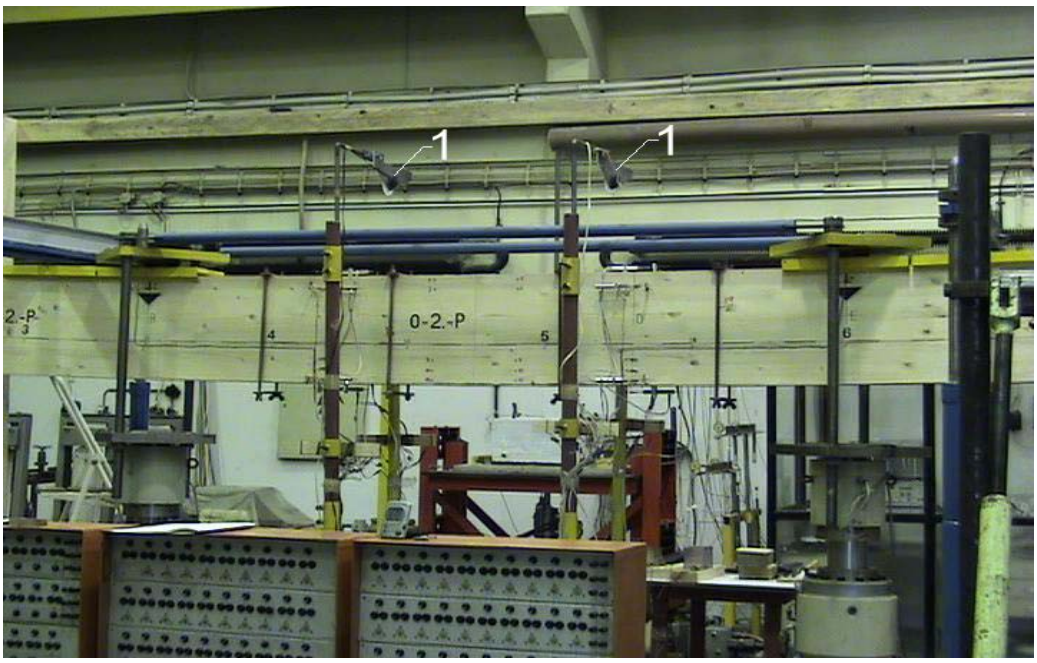

Fig. 6. Girder 0-2 close to collapse

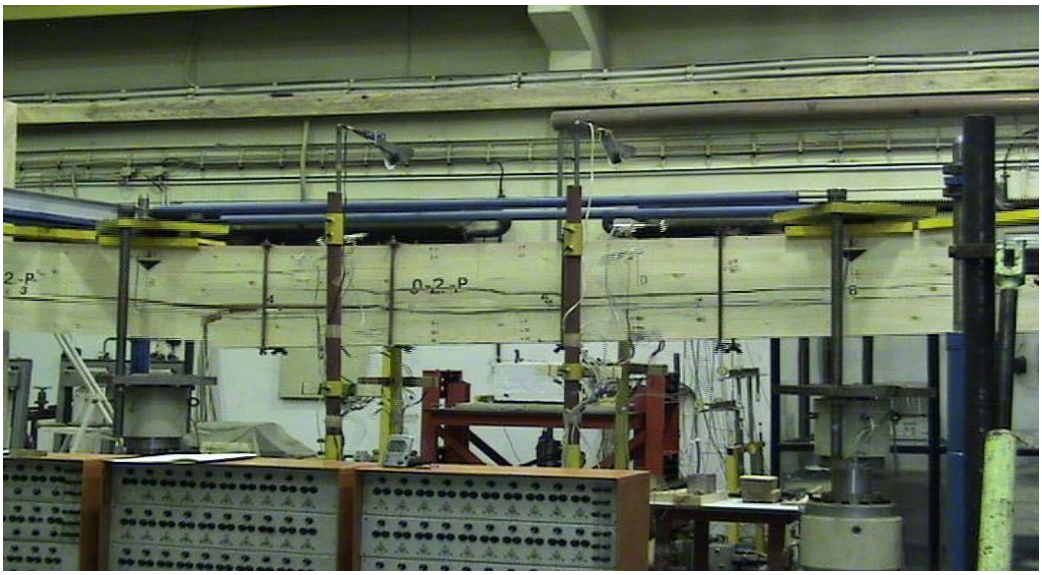

Fig. 7. Total destruction of GLULAM girder in time of 4/100 sec

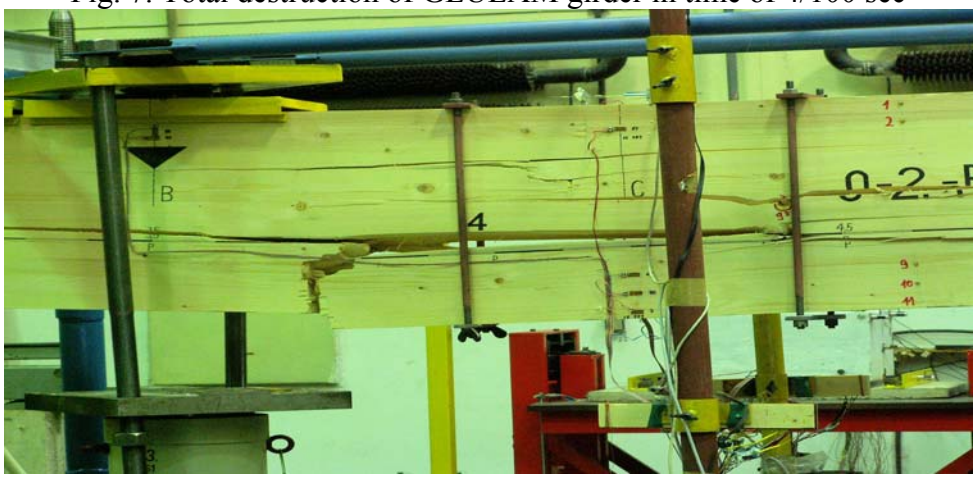

Fig. 8. Detail of destruction of girder 0-2 (GLULAM without reinforcement)

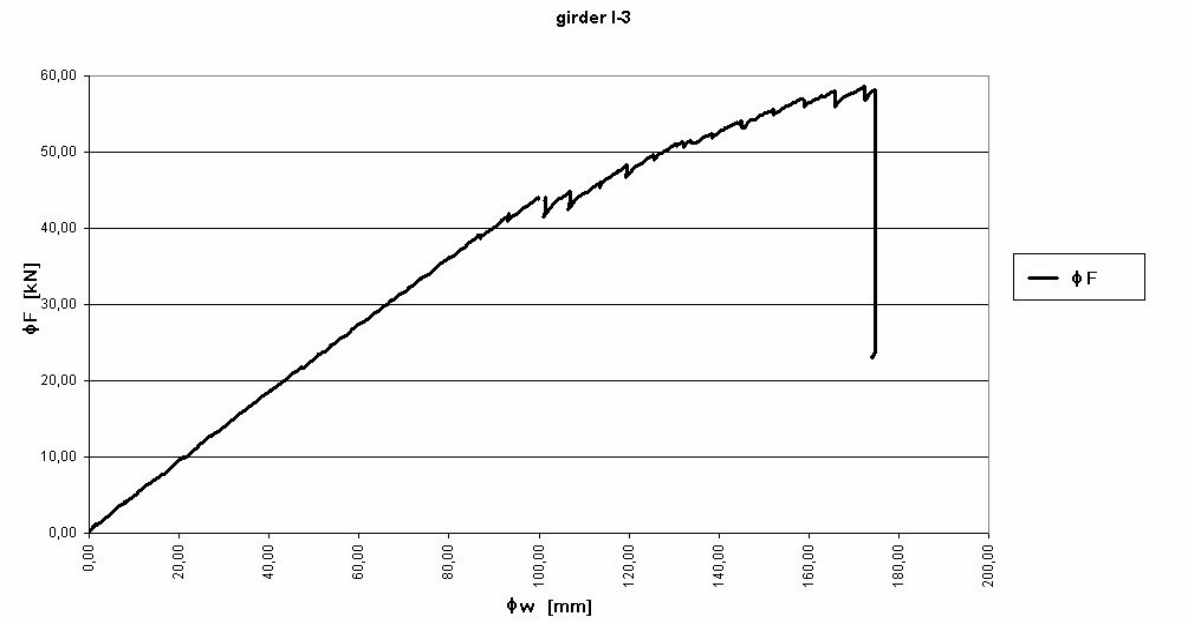

Fig. 9. Force ϕF vs deflection ϕw in girder I-3 (RELAM with reinforcement)

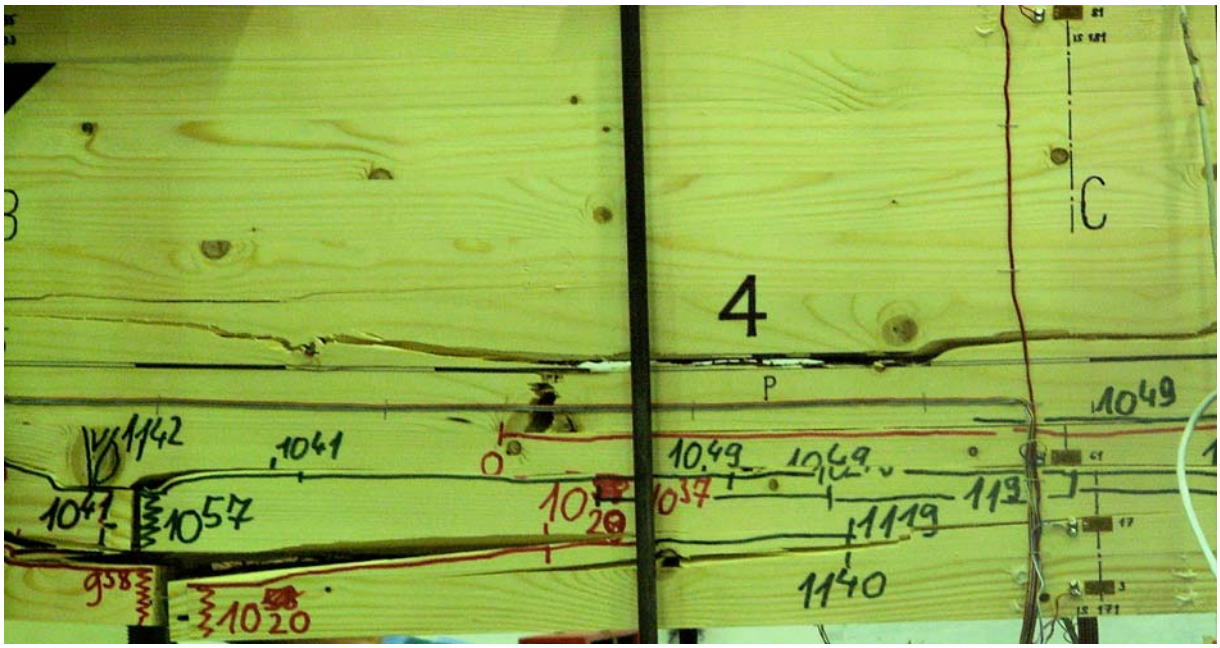

Fig. 10. Detail of girder I-3 (RELAM with reinforcement) with propagation of cracks

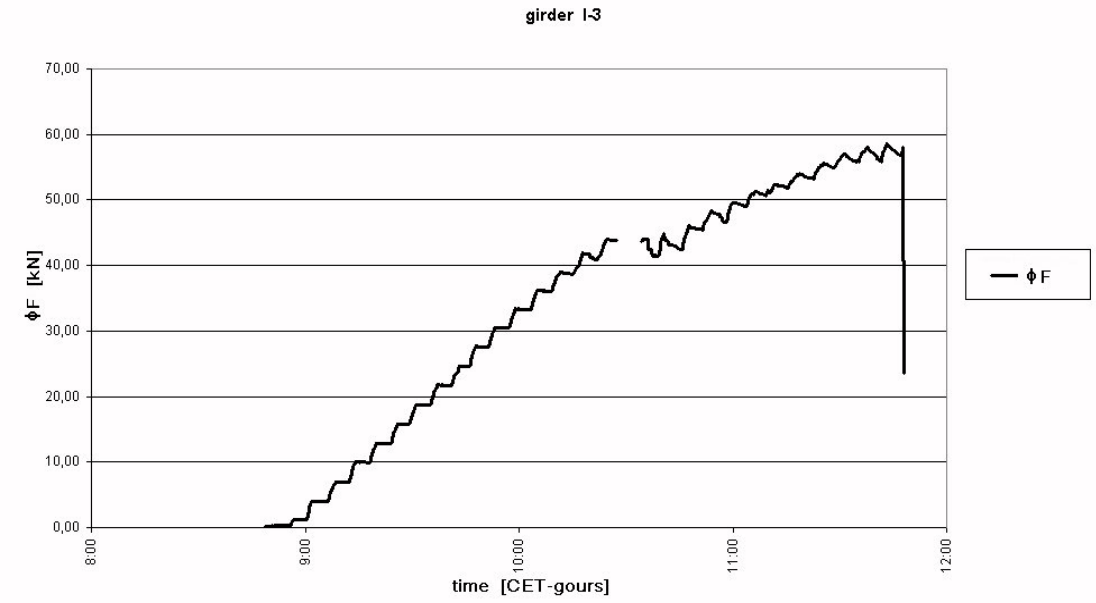

Fig. 11. Force ϕF vs time (CET) for girder I-3 with reinforcement

Girders without reinforcement (GLULAM)

Some results obtained on the girder 0-2 without reinforcement are submitted. The results are typical for the whole series of the girders without reinforcement. In Fig. 4 is plotted the function averaged force vs deflection measured 400 mm from the axis of the girder. In Fig. 5 is plotted the function averaged force vs time. In the graph are omitted data during re-installation of the loading cylinders by fixation device (see „2“ in Fig. 4). In Figs. 6 and 7 are collapse views of typical GLULAM girders. In Fig. 7 is shown the girder close to collapse. In Fig. 8 are details of the same girder under total destruction (ca. 4/100 sec after collapse).

Reinforced girders (RELAM)

Some results of reinforced RELAM girder I-3 are submitted below.

The function averaged force vs deflection is shown in Fig. 9. The destruction is specified by comparison of Figs. 4 and 9 as well as 5 and 11. Reinforced RELAM girders before obtaining the limit load present *(a) nonlinear behavior* and *(b) some increase of available load bearing capacity* as documented in Fig. 10 with detail of resulting damage and with propagation of the cracks. The time data are functions of averaged force as shown in Fig. 11.

The results obtained (see Ref. [5]) were obtained by with evaluation of the interaction of carbon fiber sheets with surrounding GLULAM-material.

5. Application

Above approaches were adopted for the design of attractive shell roof structure erected in Brezno, Slovakia (see Refs. [6] or [7]). As main structural elements were used RELAM and GLULAM arches located in longitudinal distances 6000 mm (see Figs. 12 - 15). Structural span is 60000 mm. The width of arch is 500 mm and its height varies along the length from 1800 mm in the end supports until mid-span value 780 mm. Total height and length of the structure are 22000 mm and 80000 mm, respectively.

The multi-optimization was made in order to establish the fully stressed design. All structural dimensions were optimized in accordance with such goals.

Conclusions

Some approaches for multi-functioning and multi-optimization of slender laminated wood vs carbon fiber composites were presented. The approach suggested was adopted in the analysis and design of the shell roof in Slovakia.

Fig. 12. View of the structure

Fig. 13. Another view of the structure

Fig. 14. Interior view

Fig. 15. Another interior view

References

[1] da Vinci, L.: Manuscript RL 19115v; K/P 114r, located in the Royal Library, Windsor Castle, Windsor, England, ca. 1500

[2] Felbeck, D.K. ; Atkins, A.G.: Strength and Fracture of Engineering Solids. Prentice-Hall, Inc., 1984

[3] Fox, R.L.: Optimization Methods for Engineering Design. Addison-Wesley Publishing Group, Reading, Mass., 1971

[4] Gilfillan, J.R. ; Gilbert, S.R. and Patrick, G.R.H.: The use of FRP composites in enhancing the structural behaviour of timber beams, in Journal of reinforced plastics and composites Vol.22, No.15/2003, pp.1373-1388, Sage publications, 2003

[5] Nasch, Ľ.; Tesár, A.: Limit state behavior of laminated wood girders reinforced by carbon fiber composites – Theoretical assumptions and hypothesis with experimental testing. Information for the grant APVV-99-015805, USTARCH-SAV, Bratislava, 2007

[6] Tesar, A. et al.: Ultimate response of bionics shells. Structural Engineering and Mechanics, Vol. 14, No.2 (2002), 135-150

[7] Tesar, A.: Bionics and fractal configurations in structural engineering. International Journal for Numerical Methods in Engineering, 2006, 68, 790-807

Acknowledgements

The authors are indebted to the Slovak Scientific Agency APVV for suggesting and supporting of above research in scope of scientific grant APVV-99-015805.